



## RESEARCH ARTICLE

### Isotherm, kinetic and thermodynamic studies of methylene blue adsorption using *Leucaena leucocephala*

Ali Rıza Kul<sup>1</sup> , Adnan Aldemir<sup>2,\*</sup> 

<sup>1</sup>Van Yüzüncü Yıl University, Faculty of Science, Chemistry Department, 65080, Van, TURKEY

<sup>2</sup>Van Yüzüncü Yıl University, Faculty of Engineering, Chemical Engineering Department, 65080, Van, TURKEY

## ABSTRACT

In recent years, great focused has been placed on the development of low-cost adsorbents to be used for applications regarding treatment of wastewater. In this study, *Leucaena leucocephala* peel (LLP) was used for adsorption of methylene blue from aqueous solutions. The experiments were conducted at seven concentrations (15, 30, 45, 60, 75, 90, 105 mg L<sup>-1</sup>) and three temperatures (298, 308, 318 K). The obtained data were applied to adsorption isotherm, kinetic and thermodynamic calculations. The results showed that Freundlich isotherm was more appropriate compared to Langmuir and Temkin isotherms. The kinetic results indicated that the process fitted pseudo second order model with higher R<sup>2</sup> values compared to pseudo first order and intra-particle diffusion models. Gibbs free energy, enthalpy and entropy values were calculated for 298 K as 2.776 kJ mol<sup>-1</sup>, 6.262 kJ mol<sup>-1</sup> and 11.699 J mol<sup>-1</sup>, respectively.

**Keywords:** Adsorption, isotherm, kinetic, *Leucaena leucocephala*, methylene blue, thermodynamic

## 1. INTRODUCTION

Dyes are used in variety of manufacturing such as textile, plastics, pharmaceutical, paper, printing, rubber, leather, paint, cosmetic, food and pulp [1-3]. Recently, worldwide attention has been brought to the fact that dyes, the toxic effects of which threaten the lives of humans, animals and the environment, are directly discharged into the environment [4]. Various methods have been designed to treat dye wastewater, such as adsorption [5-10], oxidation [11-12], membrane separation [13-14], electrochemical techniques [15-16] and ion exchange [17]. However, none of these methods have been successful in completely removing dyes from wastewater and all have limitations including high cost, secondary pollutant generation and poor removal efficiency. Among the different methods, adsorption has been determined as effective, low-cost and simplest process for wastewater treatment [18-20].

Activated carbon is widely used and it is the most effective adsorbent in the treatment of dyes in wastewater. However, the manufacturing and regeneration costs of activated carbon are high which is remain a major drawback [21-23]. Studies in the

literature have used various low-cost adsorbents such as Barbados shells [24], palm kernel fiber [25], cacti [26], sawdust [27], Eichhorria crassipes roots [28]. But the adsorption capacity of such adsorbents is generally quite low and it has become important to discover more cost effective, eco-friendly, efficient, renewable and abundant materials to be used as adsorbents.

Adsorption onto biochars made from land-plant residues including sawdust, weeds, corn straws, and hickory wood, has been determined as high efficient and eco-friendly option to removal dyes from wastewater [29]. Some studies have evaluated for remove capacity of dye through interactions between the dye molecule and functional groups on the surface of these adsorbents. As most land-plant residues are discarded as waste, their use as low-cost and eco-friendly adsorbents is a promising alternative.

The aim of this study was to investigate dye removal ability of *Leucaena leucocephala* peels (LLP) as a cost effective adsorbent on MB in aqueous solutions containing. MB was selected as the adsorbate as it has been found to adversely affect human health by causing different diseases [30]. Within the scope of

Corresponding Author: [adnanaldemir@yyu.edu.tr](mailto:adnanaldemir@yyu.edu.tr) (Adnan Aldemir)

Received 13 October 2020; Received in revised form 11 January 2021; Accepted 11 January 2021

Available Online 26 January 2021

Doi: <https://doi.org/10.35208/ert.810226>

© Yildiz Technical University, Environmental Engineering Department. All rights reserved.

this research, isotherm, kinetic and thermodynamic studies of the MB adsorption onto LLP was conducted.

## 2. MATERIALS AND METHOD

### 2.1. Materials

In this study, methylene blue was used as the adsorbate which formula is  $C_{16}H_{18}N_3SCl_3 \cdot 3H_2O$  (MW 319.85 g mol<sup>-1</sup>). Methylene Blue (MB), sulfuric acid (H<sub>2</sub>SO<sub>4</sub>) and sodium hydroxide (NaOH) pellets (99 %) were purchased from Merck. The stock solution 1000 mg L<sup>-1</sup> by dissolving the exact amount of MB in distilled water. The concentrations of MB solutions used for experiments were prepared by diluting the stock dye solution.

### 2.2 Adsorbent (*Leucaena leucocephala*) preparation

The *Leucaena leucocephala* peels (LLP), which were used as the adsorbent in the experiments, they were collected from the *Robinia pseudoacacia* trees that were grown on the grounds of Van Yüzüncü Yıl University, Turkey. The collected LLP were washed with distilled water and dried at 75 °C until steady weight was achieved. The dried adsorbent was then ground in a mill and divided into different size groups using a set of sieves. Samples with a particle size between 1.50 mm and 2 mm were used in experiments.

### 2.3 Adsorption experiments

In the batch experiments, which were carried out in a temperature-controlled water bath, 3 g of adsorbent was treated with 500 mL of the dye solution. The experiments were carried out at seven concentrations (15, 30, 45, 60, 75, 90, 105 mg L<sup>-1</sup>) and three temperatures (298, 308, 318 K). MB concentration in the dye solution determined over 320 min while the pH was gradually adjusted by adding H<sub>2</sub>SO<sub>4</sub> or NaOH

solutions (0.1 M). All these experiments were carried out at pH 5.5. All experiments were performed in triplicate at the same conditions and average values were used to represent for results with all the calculated data. After adsorption experiments, the concentration of MB in the solution was determined with spectrophotometer (PG Instruments, T80 model) at 660 nm wavelength. The MB concentrations were determined with a calibration curve and adsorption capacity of LLP at equilibrium was determined with Eq. (1):

$$q_e = \frac{C_0 - C_e}{m} V \quad (1)$$

where  $V$  is solution volume (L),  $C_0$  and  $C_e$  are initial and equilibrium concentrations of dye (mg L<sup>-1</sup>) and  $m$  is adsorbent mass (g). The data obtained from experiments were tested by conducting isotherm, kinetic and thermodynamic studies. The amount of adsorption at any time  $t$ ,  $q_t$  (mg g<sup>-1</sup>), was calculated by Eq. (2):

$$q_t = \frac{C_0 - C_e}{m} V \quad (2)$$

## 3. RESULTS & DISCUSSION

### 3.1. Isotherm modelling studies

In the present study, the obtained data were analyzed using Langmuir, Freundlich and Temkin models. The parameters of these models were calculated by linear form of isotherm equations. The amount of MB adsorbed per unit of LLP mass and the equilibrium concentrations in the aqueous solutions for all three temperatures are presented in Fig 1. It was determined that removal efficiency increased with increase in the initial MB concentrations. LLP adsorption capacity of MB concentration ranging from 15 to 105 mg L<sup>-1</sup> was determined as 4.785 to 36.235 mg g<sup>-1</sup> for 298 K, 5.425 to 39.025 mg g<sup>-1</sup> for 308 K and 5.545 to 40.745 mg g<sup>-1</sup> for 318 K.

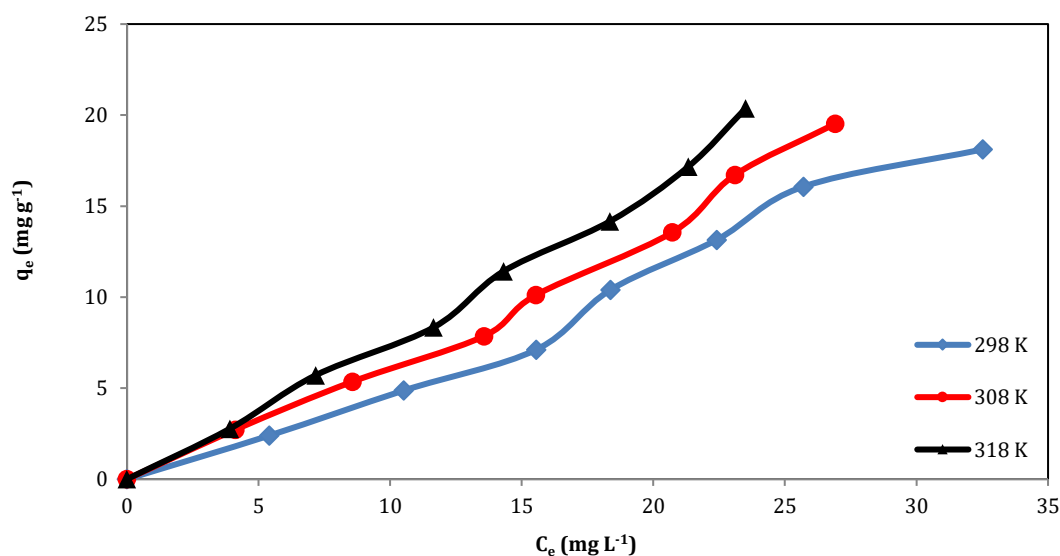


Fig 1. Adsorption isotherms for MB on the LLP at the three temperatures

Langmuir isotherm assumes monolayer coverage of the MB dye onto homogeneous adsorbent surface. Linear representation of Langmuir adsorption isotherm equation is given below:

$$\frac{C_e}{q_e} = \frac{1}{q_m K_L} + \frac{C_e}{q_m} \quad (3)$$

where  $q_m$  (mg g<sup>-1</sup>) is maximum adsorption capacity and  $K_L$  (L g<sup>-1</sup>) is Langmuir constant that can be determined from the plot of  $C_e/q_e$  versus  $C_e$ . Langmuir isotherm results of the MB adsorption onto LLP for three temperatures are given in Fig 2.

Freundlich isotherm assumes multilayer coverage of MB dye onto the heterogeneous adsorbent surface. Linear representation of Freundlich isotherm equation is presented below:

$$\ln q_e = \ln K_F + \frac{1}{n} \ln C_e \quad (4)$$

where  $K_F$  is Freundlich constant and  $n$  is heterogeneity factor.  $K_F$  and  $n$  constants are determined by plotting  $\ln q_e$  to  $\ln C_e$ . Freundlich isotherm results of MB adsorption onto LLP for three temperatures are presented in Fig 3.

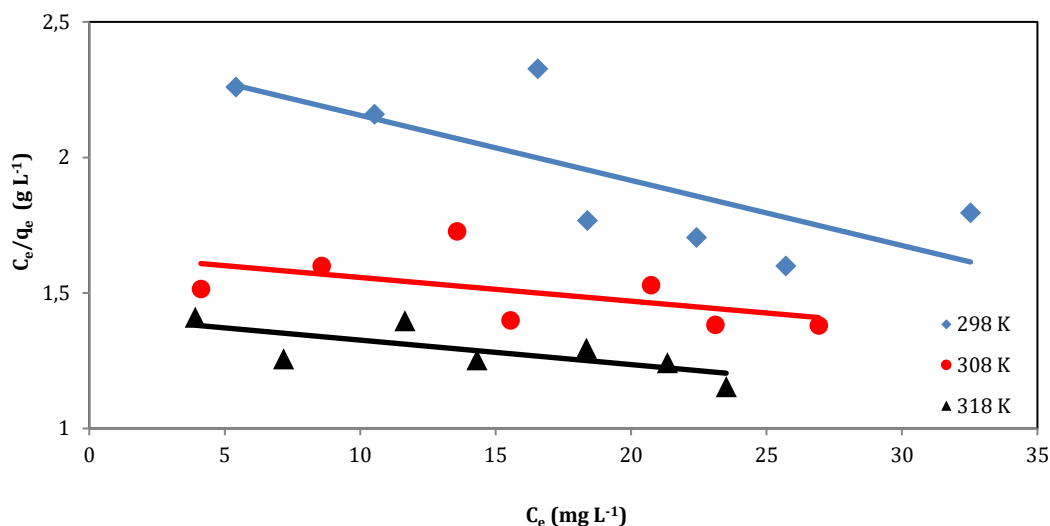


Fig 2. Langmuir adsorption isotherm for MB adsorption onto LLP

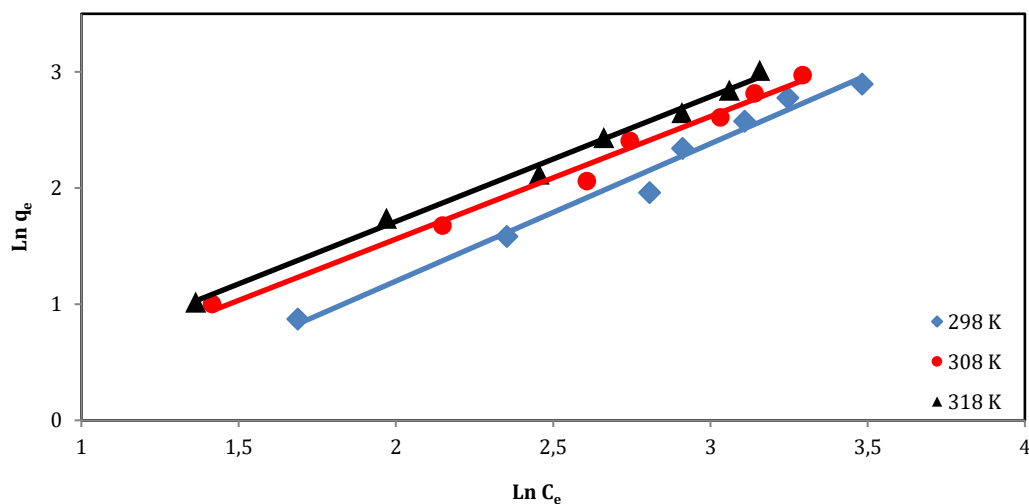


Fig 3. Freundlich adsorption isotherm for MB adsorption onto LLP

Temkin isotherm assumes decrease of adsorption heat in the layer of adsorbents that occurs due to enhancement of surface coverage of adsorbents.

$$q_e = B \ln(K_T C_e) \quad (5)$$

where  $B = RT/b_T$ ,  $T$  is absolute temperature (K),  $R$  is universal constant (J mol<sup>-1</sup> K<sup>-1</sup>) and  $K_T$  is constant (L g<sup>-1</sup>). It was determined that the increase in isotherm constants increased with increase in temperature of adsorption temperature ( $B$ ), indicating that adsorption was endothermic. Temkin

isotherm results of the MB adsorption onto LLP for three temperatures are given in Fig 4.

Table 1 clearly shows that three isotherm constants determined in this study are in comparable ranges with the values in previous studies. According to Langmuir isotherm calculations  $q_m$  and  $K_L$  values were increased with the increase of temperature which signified strong bonding between adsorbate and adsorbent.  $K_F$  and  $n$  values were increased with the rise of temperature based on the Freundlich isotherm calculations.  $K_T$  and  $b_T$  values were increased with the

increase of temperature according to Temkin isotherm calculations.  $R^2$  values of the Freundlich

model were determined to be higher than those of the other models for removal of MB using LLP.

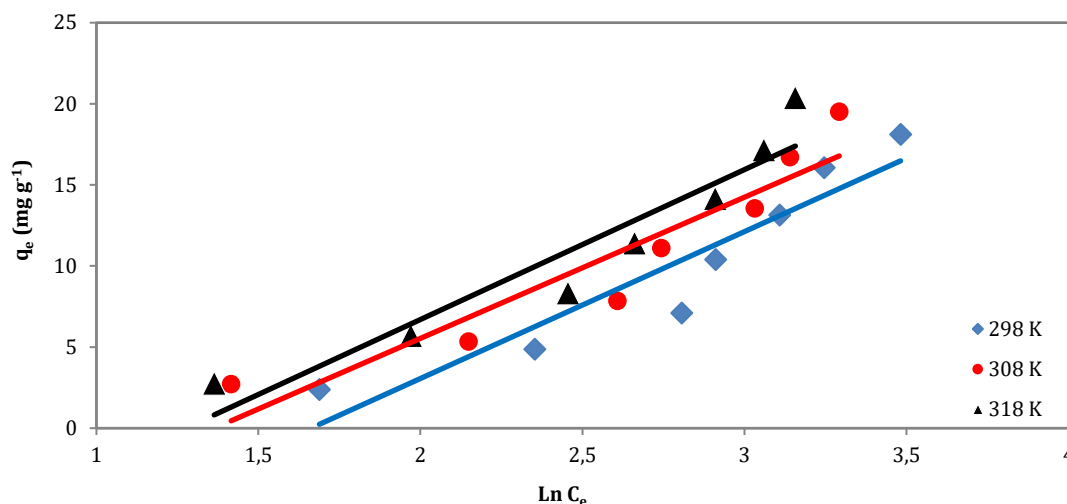


Fig 4. Temkin adsorption isotherm for MB adsorption onto LLP

Table 1. Adsorption isotherm model parameters of MB adsorption onto LLP

Temp K	Langmuir			Freundlich			Temkin		
	$K_L$ (L g <sup>-1</sup> )	$q_m$ (mg g <sup>-1</sup> )	$R^2$	$n$	$K_F$ (L g <sup>-1</sup> )	$R^2$	$K_T$ (L g <sup>-1</sup> )	$b_T$ (J mol <sup>-1</sup> )	$R^2$
298	0.0635	41.667	0.5559	0.8451	0.3106	0.9805	0.1898	273.6378	0.8847
308	0.0811	74.943	0.4969	0.9472	0.5763	0.9879	0.2557	284.2975	0.8791
318	0.1002	101.111	0.5241	0.9805	0.6455	0.9947	0.2795	296.1466	0.9032

### 3.2. Thermodynamic studies

The thermodynamic parameters, Gibbs free energy ( $\Delta G^\circ$ ), enthalpy ( $\Delta H^\circ$ ) and entropy ( $\Delta S^\circ$ ) were significant on the adsorption of MB onto LLP. These parameters were calculated using the equations given below:

$$K_d = C_{Ads}/C_e \tag{6}$$

$$\Delta G^\circ = -RT \ln K_d \tag{7}$$

$$\Delta G^\circ = \Delta H^\circ - T\Delta S^\circ \tag{8}$$

$$\ln K_d = \frac{\Delta S^\circ}{R} - \frac{\Delta H^\circ}{RT} \tag{9}$$

where  $K_d$  is the equilibrium constant. The  $\Delta H^\circ$  and  $\Delta S^\circ$  parameters were determined from plot natural logarithm of  $K_d$  versus  $1/T$  given in Fig 5. The thermodynamic parameters of MB adsorption onto LLP are listed in Table 2. The  $\Delta G^\circ$  values of this removal process were determined as  $-1359.6 \text{ J mol}^{-1}$  for 298 K,  $-1476.6 \text{ J mol}^{-1}$  for 308 K and  $-1593.6 \text{ J mol}^{-1}$  for 318 K. The  $\Delta H^\circ$  and  $\Delta S^\circ$  values of removal process of MB onto LLP were found to be  $2126.687 \text{ J mol}^{-1}$  and  $11.699 \text{ J mol}^{-1} \text{ K}^{-1}$ , respectively. The negative  $\Delta G^\circ$  values were indicated that adsorption was physisorption, which is the showed that feasibility and spontaneous nature of this process. The absolute values of  $\Delta G^\circ$  were decreased as the temperature

increased, which shows that this separation process was constructive at low temperatures. The positive  $\Delta H^\circ$  and  $\Delta S^\circ$  values were demonstrated that process endothermic and the enhanced randomness at the solid-solute interface with affinity of LLP for MB. The low enthalpy values were explained that interaction produces noncovalent bonding between dyes and adsorbents [31].

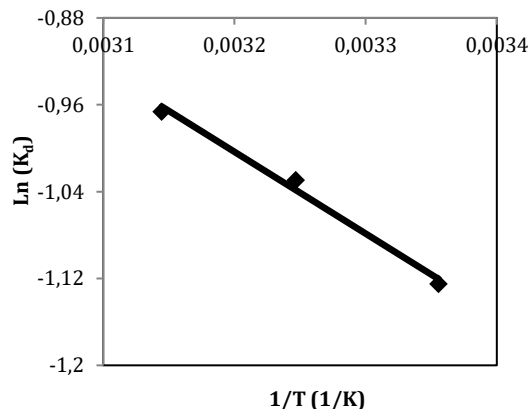


Fig 5. Van't Hoff plot for adsorption of MB onto LLP

**Table 2.** Thermodynamic parameters of adsorption of MB onto LLP

Temp (K)	$\Delta G^\circ$ (kJ mol <sup>-1</sup> )	$\Delta H^\circ$ (J mol <sup>-1</sup> )	$\Delta S^\circ$ (J mol <sup>-1</sup> K <sup>-1</sup> )	R <sup>2</sup>
298	-1.3596			
308	-1.4766	2126.687	11.699	0.9905
318	-1.5936			

**Table 3.** PFO, PSO and IPD kinetic model parameters of MB adsorption onto LLP

Kinetic Model	Temp (K)	Kinetic coefficients	15 (mg L <sup>-1</sup> )	30 (mg L <sup>-1</sup> )	45 (mg L <sup>-1</sup> )	60 (mg L <sup>-1</sup> )	75 (mg L <sup>-1</sup> )	90 (mg L <sup>-1</sup> )	105 (mg L <sup>-1</sup> )
PFO kinetic model	298	$q_e \text{ exp(mg g}^{-1}\text{)}$	4.785	9.715	14.225	20.815	26.295	32.145	36.235
	308	$q_e \text{ exp(mg g}^{-1}\text{)}$	5.425	10.715	15.715	22.225	27.135	33.445	39.025
	318	$q_e \text{ exp(mg g}^{-1}\text{)}$	5.545	11.415	16.675	22.845	28.325	34.335	40.745
	298	$k_1 \text{ (min}^{-1}\text{)}$	0.0251	0.0225	0.0276	0.0335	0.0353	0.0361	0.0379
		$q_e \text{ cal (mg g}^{-1}\text{)}$	2.5857	7.1821	8.5968	18.610	25.4598	23.6059	28.9277
		R <sup>2</sup>	0.9832	0.9441	0.9437	0.9341	0.9459	0.9269	0.9674
	308	$k_1 \text{ (min}^{-1}\text{)}$	0.0261	0.0277	0.0286	0.0313	0.0327	0.0345	0.0352
		$q_e \text{ cal (mg g}^{-1}\text{)}$	2.9544	4.5979	7.9050	11.4489	12.7866	15.9921	23.4062
		R <sup>2</sup>	0.9000	0.9112	0.9188	0.9108	0.8963	0.8786	0.9038
	318	$k_1 \text{ (min}^{-1}\text{)}$	0.0257	0.0311	0.0322	0.0361	0.0369	0.0384	0.0397
		$q_e \text{ cal (mg g}^{-1}\text{)}$	2.7442	6.9019	12.8212	12.5585	13.2381	16.7617	23.1478
		R <sup>2</sup>	0.9261	0.9314	0.9398	0.9318	0.9399	0.9226	0.9521
PSO kinetic model	298	$k_2 \text{ (min}^{-1}\text{)}$	0.0241	0.0074	0.0055	0.0044	0.0034	0.0025	0.0017
		$q_e \text{ cal (mg g}^{-1}\text{)}$	4.9529	10.5263	14.9700	18.2341	22.2221	33.7837	37.7358
		R <sup>2</sup>	0.9993	0.9961	0.9981	0.9966	0.9894	0.9982	0.9987
	308	$k_2 \text{ (min}^{-1}\text{)}$	0.0246	0.0101	0.0052	0.0049	0.0042	0.0031	0.0025
		$q_e \text{ cal (mg g}^{-1}\text{)}$	5.7077	11.1234	16.5016	23.3100	27.2486	34.8432	40.6504
		R <sup>2</sup>	0.9981	0.9997	0.9983	0.9983	0.9988	0.9988	0.9986
	318	$k_2 \text{ (min}^{-1}\text{)}$	0.0289	0.0106	0.0075	0.0069	0.0051	0.0043	0.0032
		$q_e \text{ cal (mg g}^{-1}\text{)}$	5.7241	11.8906	17.4825	23.4742	28.9017	35.2112	41.9992
		R <sup>2</sup>	0.9989	0.9988	0.9981	0.9995	0.9998	0.9996	0.9991
	298	$k_{id} \text{ (mg g}^{-1} \text{ min}^{-0.5}\text{)}$	0.1796	0.5037	0.6501	1.0127	1.2747	1.4049	1.5424
		C (mg g <sup>-1</sup> )	2.3385	2.6817	5.3859	6.9283	8.6026	12.9139	15.4132
		R <sup>2</sup>	0.6947	0.8259	0.7334	0.7801	0.8143	0.7669	0.7108
308	$k_{id} \text{ (mg g}^{-1} \text{ min}^{-0.5}\text{)}$	0.2272	0.4376	0.7049	0.9644	1.1012	1.3786	1.6116	
	C (mg g <sup>-1</sup> )	2.2898	4.8011	6.1241	9.1259	12.2371	14.7973	17.1032	
	R <sup>2</sup>	0.7734	0.6985	0.7397	0.7392	0.7084	0.7171	0.7336	
318	$k_{id} \text{ (mg g}^{-1} \text{ min}^{-0.5}\text{)}$	0.1935	0.4715	0.7371	0.8058	0.9135	1.1715	1.5801	
	C (mg g <sup>-1</sup> )	2.8841	4.9997	6.5671	12.0673	16.2435	18.7693	19.6741	
	R <sup>2</sup>	0.6774	0.7278	0.7547	0.6218	0.5623	0.6083	0.6597	

### 3.3. Adsorption kinetics studies

In this study, the MB adsorption kinetics were calculated using PFO, PSO and IPD kinetic models. The well-suited model was selected based on the regression coefficient (R<sup>2</sup>) values. These models were investigated in accordance with the experimental data obtained at varied temperatures and MB concentrations.

The PFO kinetic model is depend on the concentration of solution and solid adsorption capacity.

This model was firstly developed for characterization of liquid-solid adsorption systems depending on adsorption capacity of solid. PFO is applied to study adsorption in liquid-solid systems which have unoccupied adsorptive sites [32]. The PFO kinetic model is given in the equation below:

$$\ln(q_e - q_t) = \ln q_e - k_1 t \quad (10)$$

where  $k_1$  ( $\text{min}^{-1}$ ) is rate constant of PFO kinetic model. To achieve constants with this model, plots were drawn of  $\ln(q_e - q_t)$  against  $t$ .

The PSO kinetic model, which is explained using bond formation between the adsorptive site and solute molecule [33]. The PSO kinetic model is given in the equation below:

$$\frac{t}{q_t} = \frac{1}{(k_2 q_e^2)} + \frac{t}{q_e} \quad (11)$$

where  $k_2$  ( $\text{g mg}^{-1} \text{min}^{-1}$ ) is rate constant of PSO kinetic model. The values of  $k_2$  and  $q_e$  are identified from plot of  $t/q_t$  versus  $t$  in accordance with Equation (10).

The IPD model equation, which was proposed by Weber and Morris, is obtained by testing the possibility of IPD as the rate limiting step [34]. The IPD kinetic model is given in the equation below:

$$q_t = k_{ipd} t^{0.5} + C \quad (12)$$

where  $k_{ipd}$  ( $\text{mg g}^{-1} \text{min}^{-1/2}$ ) is IPD kinetic rate constant and  $C$  is boundary thickness. A plot of  $q_t$  against  $t^{0.5}$  at different MB concentrations gave two phases of linear plot. The PFO, PSO and IPD model parameters are given in Table 3.

The experimental results showed that the  $R^2$  coefficients were close to 1.0 which explained that this process fits the PSO kinetic model. Generally, in most dye adsorption systems the kinetic data is better represented by PSO model. In this study, the experimental and calculated  $q_e$  values for 318 K are higher than those for 298 K and 308 K. When the kinetic constants were compared, it was determined that the constant values were closer to both temperatures and concentrations for the PSO model. This result showed that the MG adsorption kinetics onto LLP confirmed the PSO model.

#### 4. CONCLUSIONS

In this study LLP were used as an adsorbent for removal of MB, a widely used dye, from aqueous solutions. Batch experiments were carried out at seven concentrations and three temperatures. LLP adsorption capacity of MB concentration ranging from 15 to 105  $\text{mg L}^{-1}$  was determined as 4.785 to 36.235  $\text{mg g}^{-1}$  for 298 K, 5.425 to 39.025  $\text{mg g}^{-1}$  for 308 K and 5.545 to 40.745  $\text{mg g}^{-1}$  for 318 K. In the isotherm model studies, experimental results showed that Freundlich isotherm model was more suitable than the other two isotherms. These isotherm coefficients increased as the temperature increased and  $R^2$  values of Freundlich model were determined to be higher than those of the other two models for removal of MB using LLP. The monolayer adsorption capacity ( $q_m$ ) of LLP was determined as 41.667 for 298 K, 74.943 for 308 K and 101.111  $\text{mg g}^{-1}$  for 318 K. This indicated that process was of an endothermic nature. The experimental data were applied to PFO, PSO and IPD kinetic models. Kinetic studies displayed that adsorption of MB process conformed the PSO model. All kinetic model coefficients increased as the temperature increased and  $R^2$  values of PSO model were higher than the other two models for removal of

MB using LLP.  $\Delta G^\circ$  values of MB adsorption onto LLP were calculated as  $-1359.6 \text{ J mol}^{-1}$  for 298 K,  $-1476.6 \text{ J mol}^{-1}$  for 308 K and  $-1593.6 \text{ J mol}^{-1}$  for 318 K.  $\Delta H^\circ$  and  $\Delta S^\circ$  values of MB adsorption onto LLP were determined to be  $2126.687 \text{ J mol}^{-1}$  and  $11.699 \text{ J mol}^{-1}$ , respectively. The experimental data showed that LLP, which is the waste of *Robinia pseudoacacia* trees, may be an alternative material to removal of dyes from wastewater.

#### REFERENCES

- [1]. S. Asad, M. A. Amoozegar, A. A. Pourbabaee, M. N. Sarbolouki and S. M. M. Dastgheib, "Decolorization of textile azo dyes by newly isolated halophilic and halotolerant bacteria," *Bioresource Technology*, Vol. 98 (11), pp. 2082–2088, 2007.
- [2]. R. L. Singh, P. K. Singh and R. P. Singh, "Enzymatic decolorization and degradation of azo dyes – a review," *International Biodeterioration & Biodegradation*, Vol. 104, pp. 21–31, 2015.
- [3]. C. Srikantan, G. K. Suraishkumar and S. Srivastava, "Effect of light on the kinetics and equilibrium of the textile dye (Reactive red 120) adsorption by helianthus annuus hairy roots," *Bioresource Technology*, Vol. 257, pp. 84–91, 2018.
- [4]. Y. Liu, Y. Liu, R. Qu, C. Ji and C. Sun, "Comparison of adsorption properties for anionic dye by metal organic frameworks with different metal ions," *Colloids and Surfaces A: Physicochemical and Engineering Aspects*, Vol. 586, pp. 1–7, 2020.
- [5]. M. A., Ahmad, N., Ahmad, N. and O. S. Bello, "Modified durian seed as adsorbent for the removal of methyl red dye from aqueous solutions," *Applied Water Science*, Vol. 5, pp. 407–423, 2015.
- [6]. A. A. Spagnoli, D. A. Giannakoudakis and S. Bashkova, "Adsorption of methylene blue on cashew nut shell based carbons activated with zinc chloride: the role of surface and structural parameters," *Journal of Molecular Liquids*, Vol. 229, pp. 465–471, 2017.
- [7]. R. Subramaniam and S. K. Ponnusamy, "Novel adsorbent from agricultural waste (cashew NUT shell) for methylene blue dye removal: optimization by response surface methodology," *Water Resources and Industry*, Vol. 11, pp. 64–70, 2015.
- [8]. M. T. Yagub, T. K. Sen, S. Afroze and H. M. Ang, "Dye and its removal from aqueous solution by adsorption: a review," *Advances Colloid and Interface Science*, Vol. 209, pp. 172–184, 2014.
- [9]. M. Rafatullah, O. Sulaiman, R. Hashim and A. Ahmad, "Adsorption of methylene blue on low-cost adsorbents: a review," *Journal of Hazardous Materials*, Vol. 177(1–3), pp. 70–80, 2010.
- [10]. M. A. M. Salleh, D. K. Mahmoud, W. A. W. A. Karim and A. Idris, "Cationic and anionic dye adsorption by agricultural solid wastes: a comprehensive review," *Desalination*, Vol. 280(1–3), pp.1–13, 2011.

- [11]. Y.-G. Kang, H. Yoon, C.-S. Lee, E.-J. Kim and Y.-S. Chang, "Advanced oxidation and adsorptive bubble separation of dyes using MnO<sub>2</sub>-coated Fe<sub>3</sub>O<sub>4</sub> nanocomposite," *Water Research*, Vol. 151, pp. 413-422, 2019.
- [12]. A. Muniyasamy, G. Sivaporul, A. Gopinath, R. Lakshmanan, A. Altaee, A. Achary and P. V. Chellam, "Process development for the degradation of textile azo dyes (mono-, di-, poly-) by advanced oxidation process - ozonation: experimental & partial derivative modelling approach," *Journal of Environmental Management*, Vol. 265, pp. 1-10, 2020.
- [13]. Y. Lu, Y. Fang, X. Xiao, S. Qi, C. Huan, Y. Zhan, H. Cheng and G. Xu, "Petal-like molybdenum disulfide loaded nanofibers membrane with super hydrophilic property for dye adsorption," *Colloids and Surfaces A: Physicochemical and Engineering Aspects*, Vol. 553, pp. 210-217, 2018.
- [14]. Y. Ma, P. Qi, J. Ju, Q. Wang, L. Hao, R. Wang and K. Sui, Y. Tan, "Gelatin/alginate composite nanofiber membranes for effective and even adsorption of cationic dyes," *Composites Part B: Engineering*, Vol. 162, pp. 671-677, 2019.
- [15]. L. A. Pereira, A. B. Couto, D. A. L. Almeida and N. G. Ferreira, "Singular properties of boron-doped diamond/carbon fiber composite as anode in Brilliant Green dye electrochemical degradation," *Diamond and Related Materials*, Vol. 103, pp. 1-7, 2020.
- [16]. N. P. Shetti, S. J. Malode, R. S. Malladi, S. L. Nargund, S. S. Shukla and T. M. Aminabhavi, "Electrochemical detection and degradation of textile dye Congo red at graphene oxide modified electrode," *Microchemical Journal*, Vol. 146, pp. 387-392, 2019.
- [17]. J. Joseph, R. C. Radhakrishnan, J. K. Johnson, S. P. Joy and J. Thomas, "Ion-exchange mediated removal of cationic dye-stuffs from water using ammonium phosphomolybdate," *Materials Chemistry and Physics*, Vol. 242, pp. 1-8, 2020.
- [18]. H. N. Bhatti, Y. Safa, S. M. Yakout, O. H. Shair, M. Iqbal and A. Nazir, "Efficient removal of dyes using carboxymethyl cellulose/ alginate/ polyvinyl alcohol/ rice husk composite: Adsorption/desorption, kinetics and recycling studies," *International Journal of Biological Macromolecules*, Vol. 150, pp. 861-870, 2020.
- [19]. C. Puri and G. Sumana, "Highly effective adsorption of crystal violet dye from contaminated water using graphene oxide intercalated montmorillonite nanocomposite," *Applied Clay Science*, Vol. 166, pp. 102-112, 2018.
- [20]. E. Alver, A. Ü. Metin and F. Brouers, "Methylene blue adsorption on magnetic alginate/rice husk bio-composite," *International Journal of Biological Macromolecules*, Vol. 154, pp. 104-113, 2020.
- [21]. F. Dhaouadi, L. Sellaoui, G. L. Dotto, A. Bonilla-Petriciolet, A. Erto and A. B. Lamine, "Adsorption of methylene blue on comminuted raw avocado seeds: Interpretation of the effect of salts via physical monolayer model," *Journal of Molecular Liquids*, Vol. 305, pp. 1-8, 2020.
- [22]. A. H. Jawad, R. Razuan, J. N. Appaturi and L. D. Wilson, "Adsorption and mechanism study for methylene blue dye removal with carbonized watermelon (*Citrullus lanatus*) rind prepared via one-step liquid phase H<sub>2</sub>SO<sub>4</sub> activation," *Surfaces and Interfaces*, Vol. 16, pp. 76-84, 2019.
- [23]. D. S. Tong, C. W. Wu, M. O. Adebajo, G. C. Jin, W. H. Yu, S. F. Ji and C. H. Zhou, "Adsorption of methylene blue from aqueous solution onto porous cellulose-derived carbon/montmorillonite nanocomposites," *Applied Clay Science*, Vol. 161, pp. 256-264, 2018.
- [24]. S. Idris, Y. A. Iyaka, M. M. Ndamitso, E. B. Mohammed and M. T. Umar, "Evaluation of kinetic models of copper and lead uptake from dye wastewater by activated pride of barbados shell," *American Journal of Chemistry*, Vol. 1, pp. 47-51, 2012.
- [25]. Y. Ho and A. Ofomaja, "Pseudo-second-order model for lead ion sorption from aqueous solutions onto palm kernel fiber," *Journal of Hazardous Materials*, Vol. 129, pp. 137-142, 2006.
- [26]. F. B. Rebah and S. M. Siddeeg, "Cactus an eco-friendly material for wastewater treatment: a review," *Journal of Materials and Environmental Science*, Vol. 8, pp. 1770-1782, 2017.
- [27]. H. A. Al-Husseiny, "Adsorption of methylene blue dye using low cost adsorbent of sawdust: batch and continues studies," *Journal of University of Babylon*, Vol. 22(2), pp. 296-310, 2014.
- [28]. W. C. Wanyonyi, J. M. Onyari and P. M. Shiundu, "Adsorption of Congo red dye from aqueous solutions using roots of *Eichhornia crassipes*: kinetic and equilibrium studies," *Energy Procedia*, Vol. 50, pp. 862-869, 2014.
- [29]. M. J. Ahmed, P. U. Okoye, E. H. Hummadi and B. H. Hameed, "High-performance porous biochar from the pyrolysis of natural and renewable seaweed (*Gelidium acerosa*) and its application for the adsorption of methylene blue," *Bioresource Technology*, Vol. 278, pp. 159-164, 2019.
- [30]. L. M. Pandey, "Enhanced adsorption capacity of designed bentonite and alginate beads for the effective removal of methylene blue," *Applied Clay Science*, Vol. 169, pp. 102-111, 2019.
- [31]. I. Ghosh, S. Kar, T. Chatterjee, N. Bar and S. K. Das, "Removal of methylene blue from aqueous solution using *Lathyrus sativus* husk: Adsorption study, MPR and ANN modeling," *Process Safety and Environmental Protection*, Vol. 149, pp. 345-361, 2021.
- [32]. S. Langergren and B. K. Svenska, "Zur theorie der sogenannten adsorption gelöster stoffe," *Veternskapsakad Handlingar*, Vol. 24, pp. 1-39, 1898.
- [33]. Y. S. Ho and G. McKay, "Kinetic models for the sorption of dye from aqueous solution by wood," *Process Safety and Environmental Protection*, Vol. 76, pp. 183-191, 1998.
- [34]. W. J. Weber and J. C. Morris, "Kinetics of adsorption on carbon from solution," *Journal of the Sanitary Engineering Division*, Vol. 89, pp. 31-60, 1963.